DIRECT TESTS OF
DYNAMICAL ELECTROWEAK SYMMETRY BREAKING[*]

E.H. Simmons, R.S. Chivukula and J. Terning

Physics Department, Boston University, 590 Commonwealth Ave.
Boston, MA, 02215, USA
E-mail: simmons@bu.edu, sekhar@bu.edu, terning@calvin.bu.edu

ABSTRACT

We review the connection between m_t and the $Zb\bar{b}$ vertex in ETC models and discuss the resulting experimental constraint on models with weak-singlet ETC bosons. We mention several recent efforts to bring ETC models into agreement with this constraint, and explore the most promising one (non-commuting ETC) in detail.

1. Introduction

Two outstanding questions in particle theory are the cause of electroweak symmetry breaking and the origin of the masses and mixings of the fermions. Because theories that use light, weakly-coupled scalar bosons to answer these questions suffer from the hierarchy and triviality problems, it is interesting to consider the possibility that electroweak symmetry breaking arises from strong dynamics at scales of order 1 TeV. This talk focuses on extended[1] technicolor[2] (ETC) models, in which both the masses of the weak gauge bosons and those of the fermions arise from gauge dynamics.

In extended technicolor models, the large mass of the top quark generally arises from ETC dynamics at relatively low energy scales. Since the magnitude of the CKM matrix element $|V_{tb}|$ is nearly unity, $SU(2)_W$ gauge invariance insures that ETC bosons coupling to the left-handed top quark couple with equal strength to the left-handed bottom quark. In particular, the ETC dynamics which generate the top quark's mass also couple to the left-handed bottom quark thereby affecting the $Zb\bar{b}$ vertex. This has been shown[3] to provide a strong experimental constraint on ETC models – particularly those in which the ETC gauge group commutes with $SU(2)_W$.

This talk begins by reviewing the connection between the top quark mass and the $Zb\bar{b}$ vertex in ETC models. The resulting experimental constraint on ETC models with weak-singlet ETC bosons is shown. Several recent attempts [4,5,6,7,8,9,10] to bring extended technicolor models into agreement with experimental data on the $Zb\bar{b}$ vertex are mentioned, and the most promising one (non-commuting ETC) is discussed.
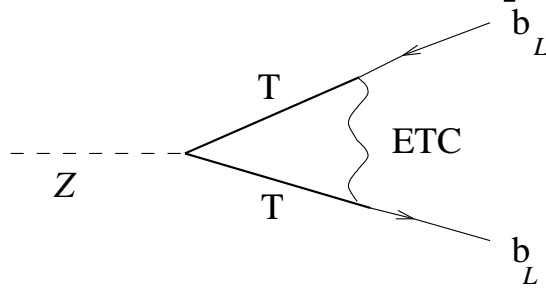
Figure 1: Direct correction to the $Z b\bar{b}$ vertex from exchange of the ETC gauge boson that gives rise to the top quark mass.

2. From m_t To A Signal of ETC Dynamics

Consider a model in which m_t is generated by the exchange of a weak-singlet ETC gauge boson of mass M_{ETC} coupling with strength g_{ETC} to the current

$$\xi \bar{\psi}_L^i \gamma^\mu T_L^{ik} + \frac{1}{\xi} \bar{t}_R \gamma^\mu U_R^k , \qquad \text{where} \quad \psi_L \equiv \begin{pmatrix} t \\ b \end{pmatrix}_L \quad T_L \equiv \begin{pmatrix} U \\ D \end{pmatrix}_L \tag{1}$$

where U and D are technifermions, i and k are weak and technicolor indices, and ξ is an ETC Clebsch expected to be of order one. At energies below M_{ETC}, ETC gauge boson exchange may be approximated by local four-fermion operators. For example, m_t arises from an operator coupling the left- and right-handed currents in Eq. (1)

$$-\frac{g_{ETC}^2}{M_{ETC}^2} \left(\bar{\psi}_L^i \gamma^\mu T_L^{iw} \right) \left(\bar{U}_R^w \gamma_\mu t_R \right) + \text{h.c.} \tag{2}$$

Assuming, for simplicity, that there is only a doublet of technifermions and that technicolor respects an $SU(2)_L \times SU(2)_R$ chiral symmetry (so that the technipion decay constant, F, is $v = 246$ GeV) the rules of naive dimensional analysis[11] give an estimate of

$$m_t = \frac{g_{ETC}^2}{M_{ETC}^2} \langle \bar{U}U \rangle \approx \frac{g_{ETC}^2}{M_{ETC}^2} (4\pi v^3) . \tag{3}$$

for the top quark mass when the technifermions' chiral symmetries break.

The ETC boson responsible for producing m_t also affects the $Z b\bar{b}$ vertex[3] when exchanged between the two left-handed fermion currents of Eq. (1) as in Fig. 1. This diagram alters the Z-boson's tree-level coupling to left-handed bottom quarks $g_L = \frac{e}{\sin\theta\cos\theta}(-\frac{1}{2} + \frac{1}{3}\sin\theta^2)$ by [3]

$$\delta g_L^{ETC} = -\frac{\xi^2}{2} \frac{g_{ETC}^2 v^2}{M_{ETC}^2} \frac{e}{\sin\theta\cos\theta} (I_3) = \frac{1}{4}\xi^2 \frac{m_t}{4\pi v} \cdot \frac{e}{\sin\theta\cos\theta} \tag{4}$$

where the right-most expression follows from applying eq. (3).

3. Comparison with the Standard Model and LEP data

To show that δg_L provides a test of ETC dynamics, we must relate it to a shift in the value of an experimental observable, and compare that shift both to radiative corrections in the standard model and to the available experimental precision.

Because ETC gives a direct correction to the $Zb\bar{b}$ vertex, we need an observable that is particularly sensitive to direct, rather than oblique[12], effects. A natural choice is the ratio of Z decay widths

$$R_b \equiv \frac{\Gamma(Z \to b\bar{b})}{\Gamma(Z \to \text{hadrons})} \tag{5}$$

because both the oblique and QCD corrections largely cancel in this ratio. One finds

$$\frac{\delta R_b}{R_b} \approx -5.1\%\xi^2 \left(\frac{m_t}{175\text{GeV}}\right). \tag{6}$$

The one-loop $Zb\bar{b}$ vertex correction in the standard model, which is largely due to exchange of longitudinal W bosons, lies in the range $[-0.5\%...-2.0\%]$[13] for 100 GeV $\geq m_t \geq 200$ GeV. The ETC-induced correction (6) is larger and in the same direction. Furthermore, because ETC models include longitudinal W bosons, the full shift in R_b in an ETC model is the sum of the W-exchange and ETC contributions.

The LEP experiments now have sufficient precision to detect such large shifts in R_b. The experimental value of $R_b = 0.2202 \pm 0.0020$ actually lies *above* the 1-loop standard model value of $R_b = 0.2155$ [15,16]. This implies that any contribution from non-standard physics is positive: $[\delta R_b/R_b]_{new} \approx +2.2\%$, thereby excluding ETC models in which the ETC and weak gauge groups commute.

4. Interlude

Having demonstrated that measurements of R_b can exclude a significant class of simple ETC models, we should check how more realistic models fare. Let us briefly review the impact of certain features of recent ETC models on the value of R_b.

A slowly-running ('walking') technicolor beta-function is often included in ETC models in order to provide the light fermions with realistically large masses, while avoiding excessive flavor-changing neutral currents[14]. Because a walking beta function enhances the size of the technifermion condensate $\langle \bar{T}T \rangle$, it leads to larger fermion masses for a given ETC scale, M_{ETC}. Enhancing m_t relative to M_{ETC} reduces the size of δg_L. However, it is has been shown [4] that the shift in R_b generally remains large enough to be visible at LEP.

It is possible to build ETC models in which the ETC coupling itself becomes strong before the scale M_{ETC} and plays a significant role in electroweak symmetry

breaking [5]. The spectrum of strongly-coupled ETC models include light composite scalars with Yukawa couplings to ordinary fermions and technifermions [6]. Exchange of the composite scalars produces corrections to R_b that are small enough to leave R_b in agreement with experiment [7]. The disadvantage of this approach is the need to fine-tune the ETC coupling close to the critical value.

ETC models also generally include 'diagonal' techni-neutral ETC bosons. The effect of these gauge bosons on R_b is discussed at length in Ref. [8]. Suffice it to say that while exchange of the diagonal ETC bosons does tend to raise R_b, this effect is significant only when the model includes large isospin violation – leading to conflict with the measured value of the oblique parameter T.

Finally, we should recall that our analysis explicitly assumed that the weak and ETC gauge groups commute. More recent work [9,10] indicates that relaxing that assumption can lead to models with experimentally acceptable values of R_b. The remainder of this talk focuses on 'non-commuting' extended technicolor models.

5. Non-commuting ETC Models

We begin by describing the symmetry-breaking pattern that enables non-commuting ETC models to include both a heavy top quark and approximate Cabibbo universality [9]. A heavy top quark must receive its mass from ETC dynamics at low energy scales; if the ETC bosons responsible for m_t are weak-charged, the weak group $SU(2)_{heavy}$ under which $(t, b)_L$ is a doublet must be embedded in the low-scale ETC group. Conversely, the light quarks and leptons cannot be charged under the low-scale ETC group lest they also receive large contributions to their masses; hence the weak $SU(2)_{light}$ group for the light quarks and leptons must be distinct from $SU(2)_{heavy}$. To approximately preserve low-energy Cabibbo universality the two weak $SU(2)$'s must break to their diagonal subgroup before technicolor dynamically breaks the remaining electroweak symmetry. The resulting symmetry-breaking pattern is :

$$
\begin{array}{rcl}
ETC & \times & SU(2)_{light} \times U(1)' \\
& \downarrow & f \\
TC \times SU(2)_{heavy} & \times & SU(2)_{light} \times U(1)_Y \\
& \downarrow & u \\
TC & \times & SU(2)_W \times U(1)_Y \\
& \downarrow & v \\
TC & \times & U(1)_{EM},
\end{array}
\tag{7}
$$

where ETC and TC stand, respectively, for the extended technicolor and technicolor gauge groups, while f, u, and $v = 246$ GeV are the expectation values of the order parameters for the three different symmetry breakings (*i.e.* the analogs of F_π for chiral symmetry breaking in QCD). Note that, since we are interested in the physics associ-

ated with top-quark mass generation, only t_L, b_L and t_R need transform non-trivially under ETC. But to ensure anomaly cancelation, it is more economical to assume that the entire third generation has the same non-commuting ETC interactions. Thus we take $(t, b)_L$ and (ν_τ, τ) to be doublets under $SU(2)_{heavy}$ but singlets under $SU(2)_{light}$, while all other left-handed ordinary fermions have the opposite $SU(2)$ assignment.

Once again, the dynamics responsible for generating the top quark's mass contributes to R_b. This time the ETC gauge boson involved transforms as a weak doublet coupling to

$$\xi \bar{\psi}_L \gamma^\mu U_L + \frac{1}{\xi} \bar{t}_R \gamma^\mu T_R \tag{8}$$

where $\psi_L \equiv (t, b)_L$ and $T_R \equiv (U, D)_R$, are doublets under $SU(2)_{heavy}$ while U_L is an $SU(2)_{heavy}$ singlet. The one-loop diagram involving exchange of this boson (analogous to Figure 1) shifts the coupling of b_L to the Z boson by

$$\delta g_L = -\frac{e}{\sin\theta\cos\theta}\frac{\xi^2 v^2}{2f^2} \approx -\frac{\xi^2}{4}\frac{e}{\sin\theta\cos\theta}\frac{m_t}{4\pi v}. \tag{9}$$

Since the tree-level $Zb_L\bar{b}_L$ coupling is also negative, the ETC-induced change tends to **increase** the coupling – and thereby increase R_b. We find that Eq. (9) results in a change to R_b of[10]

$$\frac{\delta R_b}{R_b} \approx +5.1\%\xi^2\left(\frac{m_t}{175\text{GeV}}\right). \tag{10}$$

The change is similar in size to what was obtained in the commuting ETC models, but is opposite in sign.

But that is not the full story of R_b in non-commuting ETC. Recall that there are two sets of weak gauge bosons which mix at the scale u. Of the resulting mass eigenstates, one set is heavy and couples mainly to the third-generation fermions while the other set is *nearly* identical to the W and Z of the standard model. That 'nearly' is important: it leads to a shift in the light Z's coupling to the b of order[10]

$$\delta g_L = \frac{e}{2\sin\theta\cos\theta}\frac{g_{ETC}^2 v^2}{u^2}\sin^2\alpha \tag{11}$$

where $\tan\alpha = g_{light}/g_{heavy}$ is the ratio of the $SU(2)$ gauge couplings. The couplings of the light Z to other fermions are similarly affected. When this is included, mixing alters R_b by

$$\frac{\delta R_b}{R_b} \approx -5.1\%\sin^2\alpha\frac{f^2}{u^2}\left(\frac{m_t}{175\text{GeV}}\right). \tag{12}$$

The two effects on R_b in non-commuting ETC models are of similar size and opposite sign, and their precise values are model-dependent. Thus, non-commuting ETC theories can yield values of R_b that are consistent with experiment[10].

Since R_b alone cannot confirm or exclude non-commuting ETC, we should apply a broader set of precision electroweak tests. Before doing this, we must describe

the $SU(2) \times SU(2)$ symmetry breaking sector in more detail. The two simplest possibilities for the $SU(2)_{heavy} \times SU(2)_{light}$ transformation properties of the order parameters that produce the correct combination of mixing and breaking of these gauge groups are:

$$\langle \varphi \rangle \sim (2,1)_{1/2}, \quad \langle \sigma \rangle \sim (2,2)_0 , \qquad \text{``heavy case''} \qquad (13)$$

$$\langle \varphi \rangle \sim (1,2)_{1/2}, \quad \langle \sigma \rangle \sim (2,2)_0 , \qquad \text{``light case'' .} \qquad (14)$$

Here the order parameter $\langle \varphi \rangle$ is responsible for breaking $SU(2)_L$ while $\langle \sigma \rangle$ mixes $SU(2)_{heavy}$ with $SU(2)_{light}$. We refer to these two possibilities as "heavy" and "light" according to whether $\langle \varphi \rangle$ transforms non-trivially under $SU(2)_{heavy}$ or $SU(2)_{light}$.

The heavy case, in which $\langle \varphi \rangle$ couples to the heavy group, is the choice made in [9], and corresponds to the case in which the technifermion condensation responsible for providing mass for the third generation of quarks and leptons is also responsible for the bulk of electroweak symmetry breaking. The light case, in which $\langle \varphi \rangle$ couples to the light group, corresponds to the opposite scenario in which different physics provides mass to the third generation fermions and the weak gauge bosons. While this light case is counter-intuitive (after all, the third generation is the heaviest!), it may provide a resolution to the issue of how large isospin breaking can exist in the fermion (and technifermion) mass spectrum without leaking into the W and Z masses.

We have performed a global fit for the parameters of the non-commuting ETC model (s^2, $1/x \equiv v^2/u^2$, and the δg's) to all precision electroweak data: the Z line shape, forward backward asymmetries, τ polarization, and left-right asymmetry measured at LEP and SLC; the W mass measured at FNAL and UA2; the electron and neutrino neutral current couplings determined by deep-inelastic scattering; the degree of atomic parity violation measured in Cesium; and the ratio of the decay widths of $\tau \rightarrow \mu \nu \bar{\nu}$ and $\mu \rightarrow e \nu \bar{\nu}$. Details of the calculation are reported in [10].

Table 1 compares the predictions of the standard model and the non-commuting ETC model (for particular values of $1/x$ and s^2) with the experimental values. For s^2, we have chosen a value of 0.97, at which the ETC gauge coupling is strong yet does not break the technifermion chiral symmetries by itself[10]. For $1/x$, in the heavy case we show the best fit value of $1/x = 0.0027$ or equivalently $M_W^H = 9$ TeV. The best fit for $1/x$ in the light case lies in the unphysical region of negative x but has large uncertainty: $1/x = -0.17 \pm 0.75$. For illustration, we choose a value of $1/x$ from the large range of values that give a good fit to the data; our choice, $1/x = 0.055$, corresponds to $M_W^H = 2$ TeV. We use[18,15] $\alpha_s(M_Z) = 0.115$ in these fits.

Table 2 illustrates how well non-commuting ETC models fit the precision data. This table shows the fit to the standard model for comparison; as a further benchmark we have included a fit to purely oblique corrections (the S and T parameters) [12]. The percentage quoted in the Table is the probability of obtaining a χ^2 as large or larger than that obtained in the fit, for the given number of degrees of freedom (df),

Quantity	Experiment	SM	ETC$_{\text{heavy}}$	ETC$_{\text{light}}$
Γ_Z	2.4976 ± 0.0038	2.4923	2.4991	2.5006
R_e	20.86 ± 0.07	20.73	20.84	20.82
R_μ	20.82 ± 0.06	20.73	20.84	20.82
R_τ	20.75 ± 0.07	20.73	20.74	20.73
σ_h	41.49 ± 0.11	41.50	41.48	41.40
R_b	0.2202 ± 0.0020	0.2155	0.2194	0.2188
A_{FB}^e	0.0156 ± 0.0034	0.0160	0.0159	0.0160
A_{FB}^μ	0.0143 ± 0.0021	0.0160	0.0159	0.0160
A_{FB}^τ	0.0230 ± 0.0026	0.0160	0.0164	0.0164
$A_\tau(P_\tau)$	0.143 ± 0.010	0.146	0.150	0.150
$A_e(P_\tau)$	0.135 ± 0.011	0.146	0.146	0.146
A_{FB}^b	0.0967 ± 0.0038	0.1026	0.1026	0.1030
A_{FB}^c	0.0760 ± 0.0091	0.0730	0.0728	0.0730
A_{LR}	0.1637 ± 0.0075	0.1460	0.1457	0.1460
M_W	80.17 ± 0.18	80.34	80.34	80.34
M_W/M_Z	0.8813 ± 0.0041	0.8810	0.8810	0.8810
$g_L^2(\nu N \to \nu X)$	0.3003 ± 0.0039	0.3030	0.3026	0.3030
$g_R^2(\nu N \to \nu X)$	0.0323 ± 0.0033	0.0300	0.0301	0.0300
$g_{eA}(\nu e \to \nu e)$	-0.503 ± 0.018	-0.506	-0.506	-0.506
$g_{eV}(\nu e \to \nu e)$	-0.025 ± 0.019	-0.039	-0.038	-0.039
$Q_W(Cs)$	-71.04 ± 1.81	-72.78	-72.78	-72.78
$R_{\mu\tau}$	0.9970 ± 0.0073	1.0	0.9946	1.0

Table 1: Experimental [15,16,17] and predicted values of observables for the standard model and non-commuting ETC model (heavy and light cases) for $\alpha_s(M_Z) = 0.115$, and $s^2 = 0.97$. For the heavy case $1/x$ assumes the best-fit value of 0.0027; for the light case, $1/x$ is set to 0.055. The standard model values correspond to the best fit (with $m_t = 173$ GeV, $m_{\text{Higgs}} = 300$ GeV) in [15], corrected for the change in $\alpha_s(M_Z)$, and the revised extraction [19] of $\alpha_{em}(M_Z)$.

Model	χ^2	df	$\chi^2/$df	probability
SM	33.8	22	1.53	5%
SM+S,T	32.8	20	1.64	4%
ETC$_{\text{light}}$	22.6	20	1.13	31%
ETC$_{\text{heavy}}$	20.7	19	1.09	36%

Table 2: The best fits for the standard model, beyond the standard model allowing S and T to vary, and the non-commuting ETC models. Inputs: $\alpha_s(M_Z) = 0.115$, $s^2 = 0.97$ (both ETC models), and $1/x = 0.055$ (light case). χ^2 is the sum of the squares of the difference between prediction and experiment, divided by the error.

Model	χ^2	df	χ^2/df	probability
SM	27.8	21	1.33	15%
SM+S,T	27.7	20	1.38	12%
ETC$_{\text{light}}$	25.0	20	1.25	20%
ETC$_{\text{heavy}}$	22.3	19	1.17	27%

Table 3: The best fits for the standard model, beyond the standard model allowing S and T to vary, and the non-commuting ETC model. The inputs are: $\alpha_s(M_Z) = 0.124$, $s^2 = 0.97$, and for the light case $1/x = 0.055$.
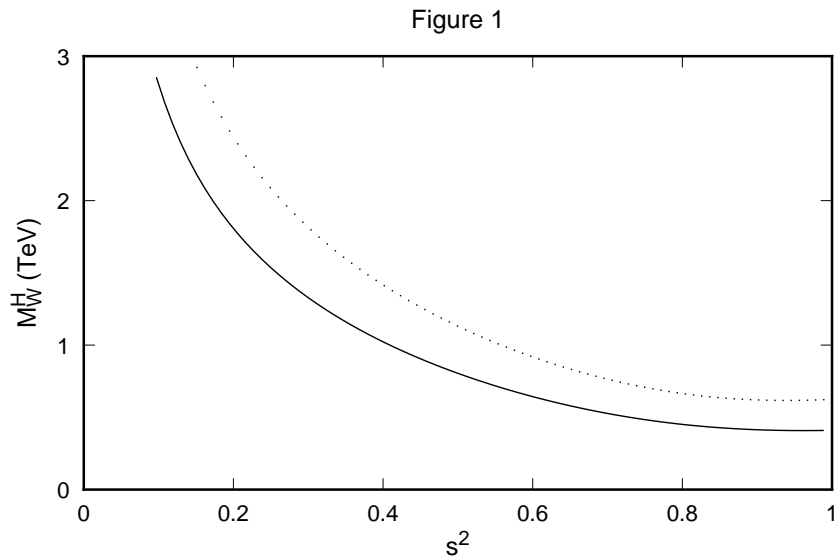

Figure 2: Lower bound on M_W^H at 95% c.l. (solid line) and 68% c.l. (dotted line) as a function of s^2 for the light case (using $\alpha_s(M_Z) = 0.115$)

assuming that the model is correct. A small probability corresponds to a poor fit. The $SM+S,T$ fit shows that merely having more parameters does not ensure a better fit.

From Tables 1 and 2 we see that because non-commuting ETC models accommodate changes in the Z partial widths, they give a significantly better fit to the experimental data than the standard model does, even after taking into account that in the fitting procedure the non-commuting ETC models have two extra parameters. In particular non-commuting ETC predicts values for Γ_Z, R_e, R_μ, R_τ, and R_b that are closer to experiment than those predicted by the standard model.

For comparison we also performed the fits using[15] $\alpha_s(M_Z) = 0.124$, as summarized in Table 3. While the standard model fit improves for a larger value of $\alpha_s(M_Z)$, the light case of the non-commuting ETC model remains a better fit.

As a bonus, the extra W and Z bosons can be relatively light. Figure 2 displays

the 95% and 68% confidence level lower bounds (solid and dotted lines) on the heavy W mass (M_W^H) for different values of s^2 (with $\alpha_s(M_Z) = 0.115$). The plot was created as follows: for each value of s^2 we fit to the three independent parameters (δg_L^b, $\delta g_L^\tau = \delta g_L^{\nu_\tau}$, and $1/x$); we then found the lower bound on x and translated it into a lower bound on the heavy W mass. Note that for $s^2 > 0.85$, the heavy W gauge boson can be as light as 400 GeV. In the heavy case, similar work shows that the lowest possible heavy W mass at the 95% confidence level is ≈ 1.6 TeV, for $0.7 < s^2 < 0.8$.

6. Conclusions

The $Zb\bar{b}$ vertex is sensitive to the dynamics that generates the top quark mass. As such, it provides an excellent test of extended technicolor models. Measurements of R_b at LEP have already excluded ETC models in which the ETC and weak gauge groups commute. Models in which ETC gauge bosons carry weak charge can give experimentally allowed values of R_b because contributions to the $Zb\bar{b}$ vertex from ZZ' mixing are similar in magnitude and opposite in sign to those from exchange of the ETC boson that generates the top quark's mass. These non-commuting ETC models can actually fit the full set of precision electroweak data better than the standard model.

1. S. Dimopoulos and L. Susskind, *Nucl. Phys.* **B155** (1979) 237; E. Eichten and K. Lane, *Phys. Lett.* **B90** (1980) 125.
2. S. Weinberg, *Phys. Rev.* **D13** (1976) 974 and **D19** (1979) 1277; L. Susskind, *Phys. Rev.* **D20** (1979) 2619.
3. R.S. Chivukula, S.B. Selipsky, and E.H. Simmons, *Phys. Rev. Lett.* **69** (1992) 575.
4. R.S. Chivukula, E. Gates, E.H. Simmons, and J. Terning, *Phys. Lett.* **B311** (1993) 383. hep-ph/9305232.
5. T. Appelquist, M. Einhorn, T. Takeuchi, and L.C.R. Wijewardhana, *Phys. Lett.* **220B**, 223 (1989); V.A. Miransky and K. Yamawaki, *Mod. Phys. Lett.* **A4** (1989) 129; K. Matumoto *Prog. Theor. Phys. Lett.* **81** (1989) 277.
6. R. S. Chivukula, K. Lane, and A. G. Cohen, *Nucl. Phys.* **B 343** (1990) 554; T. Appelquist, J. Terning, and L. Wijewardhana, *Phys. Rev* **44** (1991) 871. E.H. Simmons, *Nucl. Phys.* **B312** (1989) 253.
7. N. Evans, *Phys. Lett.* **331** (1994) 378, hep-ph/9403318; C.D. Carone, E.H. Simmons, and Y. Su. *Phys. Lett.* **B344** 287 (1995), hep-ph/9410242.
8. T. Yoshikawa, *Mod. Phys. Lett* **A10** (1995) 1601, hep-ph/9411280; G.-H. Wu, *Phys. Rev. Lett.* **74** (1995) 4137, hep-ph/9412206; K. Hagiwara and N. Kitazawa, hep-ph/9504332; C.-X. Yue, Y.P. Kuang, G.-R. Lu, L.-D. Wan, hep-ph/9506480.

9. R.S. Chivukula, E.H. Simmons, and J. Terning, hep-ph/9404209, *Phys. Lett.* **B331** (1994) 383.

10. R.S. Chivukula, E.H. Simmons, and J. Terning, hep-ph/9506427.

11. A. Manohar and H. Georgi, *Nucl. Phys.* **B234** (1984) 189.

12. B. Lynn, M. Peskin, and R. Stuart, in *Physics at LEP*, J. Ellis and R. Peccei eds. CERN preprint **86-02** (1986). M. Golden and L. Randall, *Nucl. Phys.* **B361**, 3 (1991); B. Holdom and J. Terning, *Phys. Lett* **B247**, 88 (1990); M. Peskin and T. Takeuchi, *Phys. Rev. Lett.* **65**, 964 (1990); A. Dobado, D. Espriu, and M. Herrero, *Phys. Lett.* **B253**, 161 (1991); M. Peskin and T. Takeuchi *Phys. Rev.* **D46** 381 (1992).

13. A.A. Akhundov, D.Yu. Bardin and T. Riemann, *Nucl. Phys.* **B2**76 (1986) 1 ; W. Beenakker and W. Hollik, Z. Phys. C40 (1988) 141; J. Bernabeu, A. Pich and A. Santamaria, *Phys. Lett.* **B2**00 (1988) 569 ; B.W. Lynn and R.G. Stuart, *Phys. Lett.* **B2**52 (1990) 676.

14. B. Holdom, *Phys. Lett.* **B105** (1985) 301; K. Yamawaki, M. Bando and K. Matumoto, *Phys. Rev. Lett.* **56** (1986) 1335; V.A. Miransky, *Nuovo Cim.* **90A** (1985); T. Appelquist, D. Karabali, and L.C.R. Wijewardhana, *Phys. Rev.* **D35**(1987) 389; 149; T. Appelquist and L.C.R Wijewardhana, *Phys. Rev.* **D35** (1987) 774; *Phys. Rev.* **D36** (1987) 568.

15. P. Langacker, hep-ph/9408310; see also P. Langacker and J. Erler, http://www-pdg.lbl.gov/rpp/book/page1304.html, *Phys. Rev.* **D50** (1994) 1304.

16. A.Blondel, http://alephwww.cern.ch/ALEPHGENERAL/reports/reports.html, CERN PPE/94-133.

17. Particle Data Group, *Phys. Rev.* **D 50** (1994); See also A. Pich and J.P. Silva hep-ph/95-5327, FTUV/95-21, IFIC/95-21.

18. C.T.H. Davies et. al., hep-ph/9408328, OHSTPY-HEP-T-94-013, FSU-SCRI-94-79; I. Hinchliffe, http://www-pdg.lbl.gov/rpp/book/page1297.html, *Phys. Rev.* **D50** (1994) 1297; M. Virchaux, Saclay preprint, DAPHNIA/SPP 92-30, presented at the "QCD 20 years later" workshop, Aachen Germany, (1992); R. Voss, in *Proceedings of the 1993 International Symposium on Lepton and Photon Interactions at High Energies*, Ithaca NY (1993).

19. M. Swartz, hep-ph/9411353, SLAC-PUB-6710; see also A.D. Martin and D. Zeppenfeld, hep-ph/9411377, MADPH-94-855; S. Eidelman and F. Jegerlehner, hep-ph/9502298, PSI-PR-95-1.